Organic & Biomolecular Chemistry

RSC Publishing

PAPER

View Article Online
View Journal | View Issue

Cite this: *Org. Biomol. Chem.*, 2013, **11**, 4006

A 'dual click' strategy for the fabrication of bioselective, glycosylated self-assembled monolayers as glycocalyx models†

Carsten Grabosch,[a] Martin Kind,[b] Yasmin Gies,[b] Felix Schweighöfer,[b] Andreas Terfort*[b] and Thisbe K. Lindhorst*[a]

Received 22nd February 2013,
Accepted 12th April 2013

DOI: 10.1039/c3ob40386f

www.rsc.org/obc

Solid surfaces decorated with specific saccharide patterns can serve as a model for the chemically and structurally highly complex glycocalyx of eukaryotic cells. Here we present an approach based on self-assembled monolayers on gold, which are built up in a three-step manner to provide a solid basis, a biorepulsive oligoethylene glycol part, and a specific carbohydrate terminus in a modular way. Of the different reaction sequences, the one with two consecutive 'click reactions' (the copper(I)-catalysed 1,3-dipolar cycloaddition of alkynes with azides and the thiourea-bridging of isothiocyanates with amines) directly 'on SAM' results in the densest layers, as demonstrated by infrared absorption reflection spectroscopy and ellipsometry. As a 'real life' test, the surfaces obtained this way were used for bacterial adhesion experiments. Here the biorepulsivity of the middle part of the SAMs as well as specific binding to the carbohydrate termini could be clearly demonstrated.

Introduction

Eukaryotic cells are covered by a nanometre-thick molecular layer that consists of a complex multitude of structurally very diverse glycoconjugates. This so-called glycocalyx is of essential importance for fundamental biochemical processes such as cell–cell communication and cell adhesion.[1] To study the details of the molecular recognition processes occurring at the glycosylated cell surface, suitable synthetic models are required.[2] These ideally allow for the construction of defined glycoarrays and their structural modification on demand. Thus, many different glycoarrays and methods for the preparation of carbohydrate-coated surfaces have been introduced.[3] However, among the different types of glycoarrays that are used in glycobiology, systems based on glycosylated self-assembled monolayers (glyco-SAMs) have unique advantages.[4] SAMs offer the possibility to fabricate reliable as well as structurally diverse, well-ordered glycoarrays,[5] in particular when systems with long alkyl chains at the basis are used.[6] With regard to the well-defined monolayer which is formed in the self-assembly process, glyco-SAMs are unmatched by any other glycoarray concepts regarding the regularity and controllability of the formed monolayer. In addition, SAMs are amenable to a number of biophysical methods that facilitate their characterisation, and the precise investigation of molecular interactions with the SAM surface.[7]

The most frequently used class of SAMs are thiolate monolayers on gold, which are conveniently formed by immersion of gold substrates in solutions of thiols,[8] thioacetates,[9] or disulphides,[10] respectively. For biological adhesion studies, it is essential to use so-called biorepulsive SAMs, which suppress the unspecific adsorption of proteins to the surface. Such protein-repelling properties can be achieved by the introduction of oligoethylene glycol (OEG) moieties into the employed molecules.[11] Biorepulsive properties of glyco-SAMs are a prerequisite for the investigation of carbohydrate recognition by specific proteins, called lectins.[12]

Lectins occur ubiquitously in all organisms, but serve very different functions. In vertebrates they play essential roles in cell–cell recognition and signalling,[13] while microorganisms on the other hand utilise own lectins to attach to the glycocalyx of their host cells.[14] For example, pathogenic bacteria such as UPEC (uropathogenic *Escherichia coli*) utilise fimbrial lectins to adhere to glycosylated surfaces and eventually form biofilms.[15] These bacterial adhesion and colonisation processes can cause severe infections,[16] which are often life-threatening especially for young children. It is therefore important to study and

[a]*Otto Diels Institute of Organic Chemistry, Christiana Albertina University of Kiel, Otto-Hahn Platz 3/4, D-24098 Kiel, Germany. E-mail: tklind@oc.uni-kiel.de; Fax: +49 431 880 7410; Tel: +49 431 880 2023*
[b]*Institute of Inorganic and Analytic Chemistry, Goethe-University Frankfurt, D-60438 Frankfurt, Germany. E-mail: aterfort@chemie.uni-frankfurt.de; Fax: +49 69 798 29188; Tel: +49 69 798 29180*
†Electronic supplementary information (ESI) available. See DOI: 10.1039/c3ob40386f

understand the details of fimbriae-mediated, carbohydrate-specific bacterial adhesion, in order to develop antiadhesive surfaces, such as for transplantation medicine, and means for prevention of bacterial adhesion.[17]

Hence it has become our goal to utilise glyco-SAMs to study carbohydrate-specific bacterial adhesion employing live *E. coli* cells. Owing to our expertise with type 1-fimbriated *E. coli*, a respective GFP-tagged strain (pPKL1162) was employed.[18] In this fluorescent strain, some hundred copies of type 1 fimbriae are projected from the bacterial surface. They carry an α-D-mannoside-specific lectin at their tips, called FimH. So far, FimH is the best-investigated bacterial lectin involved in bacterial adhesion.[19] Its structure and carbohydrate specificity are well understood from several X-ray studies.[20]

To achieve a selective recognition of a surface by these entities, it is necessary not only to expose α-D-mannoside residues, but also to tailor the surface in such a way that the non-specific adhesion of this and other proteins becomes suppressed. In principle, this is possible by the synthesis of a molecule consisting of three blocks, that is (1) a mercaptoalkyl chain (for the formation of a stable SAM), (2) an OEG chain (for the suppression of non-specific interactions), and (3) an α-D-mannoside terminus (for the specific interaction with the bacterial lectin). During an optimisation project, this would require many multi-step syntheses of the different molecules, so we rather wished to develop a convergent strategy to assemble all the required molecular parts directly at the surface ('on SAM' synthesis).

We have recently started to elaborate a 'dual click' concept for the formation of glyco-SAMs.[21] This approach combines two orthogonal, chemoselective reactions with 100% atom economy: first, the classical 'click reaction' of azides and alkynes in the presence of Cu(I) yielding triazole ligation products,[22] and second, thiourea-bridging, conjugating an amine and an isothiocyanate by formation of a thiourea bridge, catalysed by a tertiary amine. Here we show for the first time that by such a strategy, three key achievements for a powerful glycobiological tool can be accomplished: (i) fabrication of biorepulsive glyco-SAMs with inherent structural variability through a 'dual click' chemoselective ligation chemistry, which can be performed 'on SAM' (Scheme 1); (ii) monitoring of all construction steps by characterisation of the resulting SAM systems *via* ellipsometry and infrared absorption reflection spectroscopy (IRRAS); and (iii) demonstration of stability and selectivity of the achieved glyco-SAMs for the study of carbohydrate-specific adhesion with live *E. coli* cells.

Results and discussion

Synthesis of the building blocks and test of the 'click reactions' in solution

All reactions were performed in homogeneous solution to elaborate the coupling chemistry. Optimised reaction conditions were then transferred to the construction of the bioselective glycol-SAMs. Since free thiols interfere *e.g.* with the Cu(I)-mediated 'click chemistry', we decided to protect the thiol groups. Several protective groups permitting the formation of thiolate-anchored SAMs on gold surfaces for thiols exist. Here the acetyl group was selected. The thioacetate-functionalised alkyne **1** has been used in a previous study both for the formation of SAMs and for 'click reactions' in solution.[21b] Here it was also used to optimise the 'click reactions' in solution before transferring them to the surface. For the Cu(I)-catalysed 1,3-dipolar cycloaddition reaction, the difunctional amino-hexaethylene glycol azide was employed, since it provides the biorepulsive OEG unit later to be used in the SAMs. Surprisingly, the desired amino-terminated 1,4-triazole **2** could only be obtained in 46% yield even under optimised conditions. The reason for this relatively low yield is a migration of the *S*-acetyl group towards the amino group under the reaction conditions (*cf.* ESI†). The second 'click reaction' was performed between the amine **2** and the *p*-isothiocyanato-functionalised mannoside **3**.[23] Under optimised reaction conditions (diisopropylethylamine (DIPEA) in DMF), the thiourea-bridged thioacetate **4** could be obtained in a pure form and excellent yield (Scheme 2).

To avoid the problems with $S \rightarrow N$-acetyl group migration, we switched to the corresponding disulphides, which can be regarded as self-masked thiols, capable of forming thiol monolayers of comparable quality as the ones derived from thiols.[5b] For this, commercially available 11-mercaptoundecanoic acid was oxidatively dimerised by treatment with sulphuryl chloride to form **5**.[10b]

Disulphide **5** was coupled with propargylamine using a 2-(7-aza-1*H*-benzotriazole-1-yl)-1,1,3,3-tetramethyluronium hexafluoro-phosphate (HATU)-mediated amide coupling reaction to form alkyne amide **6** (Scheme 3). 'Click reaction' with amino-hexaethylene glycol azide in degassed methanol using copper(I) iodide yielded 78% of the bistriazole **7**. DMF turned out to be unsuitable for the thiourea conjugation – the second 'click reaction' – of the disulphide system. Instead disulphide **7** was dissolved in a small amount of DMSO. Addition of THF and a catalytic amount of DIPEA gave the thiourea-bridged disulphide **8** in 62% yield after heating the mixture to 40 °C for 48 h.

After the reaction conditions for both 'click reactions' were optimised in solution, we tried to transfer these protocols to the surface reactions.

Construction of the bioselective glyco-SAMs by 'dual click' reactions

For the deposition of the SAMs, both disulphides and thioacetates have been employed. When deposited from ethanol, both kinds of molecules form similar thiolate SAMs on gold.[5a] In this study, typically the thioacetates were preferred due to their better solubilities. A notable exception was the formation of the amino-terminated SAM (step C in Scheme 1), for which the disulphide **7** was preferred over the thioacetate **2**, since we found spectroscopic hints for migration of the *S*-acetyl group on the surface, too (*cf.* ESI†). These layers can also be prepared by the 'on SAM click reaction' of the monolayers formed from

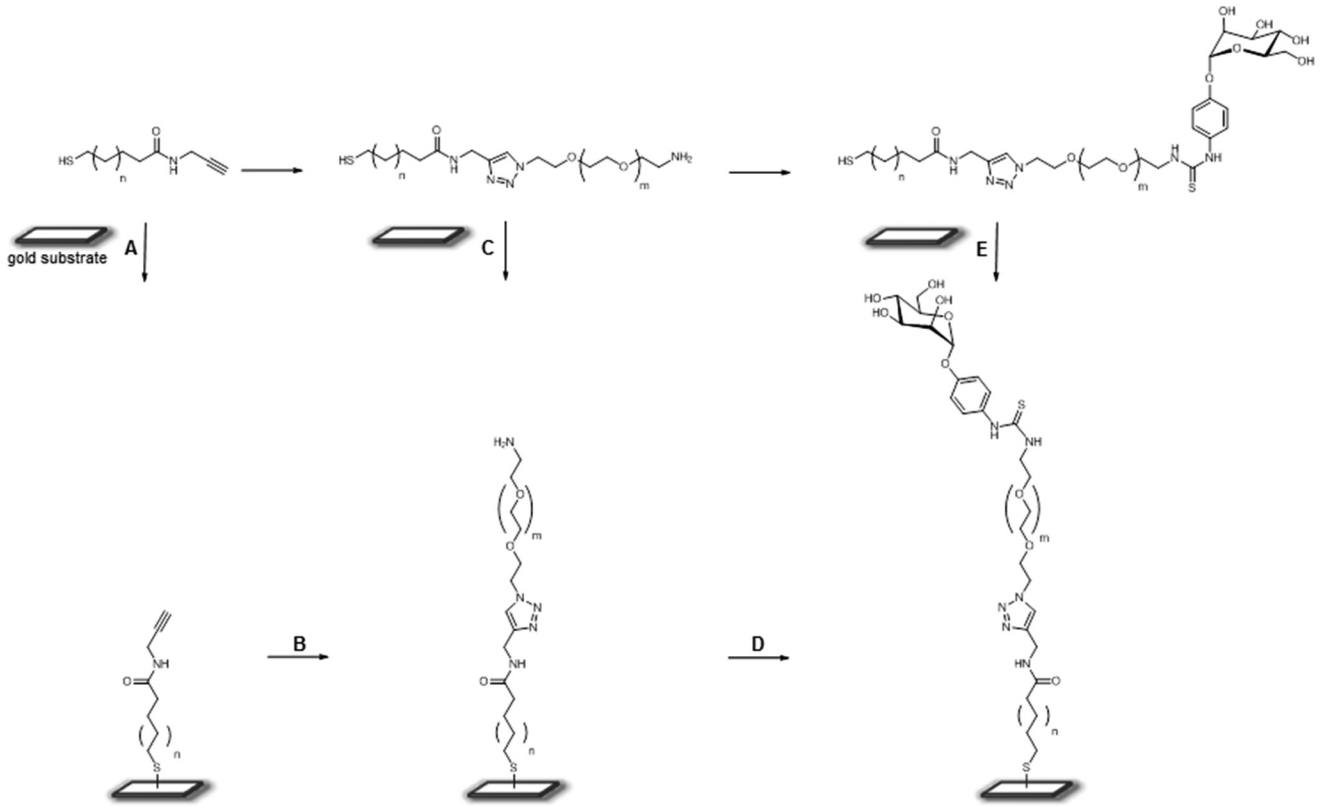

Scheme 1 Outline of the formation of glyco-SAMs by the 'dual click' approach either in solution, 'on SAM', or a combination thereof. The 'dual click' approach facilitates the fabrication of many different biorepulsive glyco-SAMs by using a kit-like combination of building blocks. Note that the mannosyl residue, which has been used in this work, represents a whole group of possible carbohydrate residues.

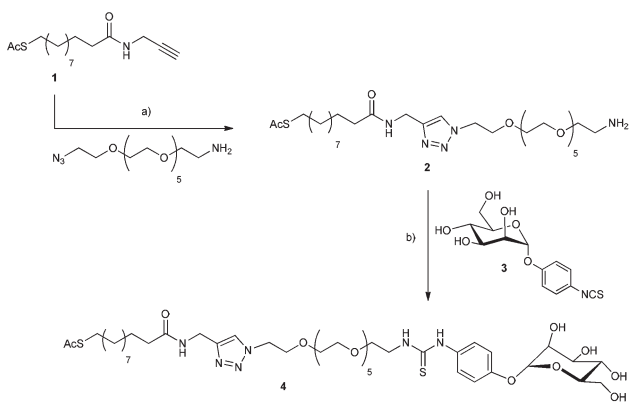

Scheme 2 Synthesis of amino-functionalised thioacetate **2** and thiourea-bridging in solution. (a) CuI, MeCN, 45 °C, 24 h, 46%; (b) DIPEA, DMF, rt, 12 h, quant.

alkyne **1** with the OEG azide following a protocol established by us earlier (step B in Scheme 1).[21b] This led to layers of **7** which were characterised by ellipsometry and IRRAS. Fig. 1 compares the spectra of the bulk substance **7** (trace a) and the one obtained from the surface (trace b).

Spectra a and b (Fig. 1) resemble each other in all major bands, thus indicating that a monolayer of **7** has been formed on the Au surface (for the detailed assignments of the bands see Table S1 in the ESI†). Ellipsometry measurements with the SAM formed with **7** yielded a layer thickness of 30 ± 2 Å. Applying standard bond lengths, the maximum length of molecule **7** can be approximated to be 44 Å. Thus, the determined layer thickness is in line with the assumption that a thiolate monolayer has formed from the amino-terminated disulphide. An experimental layer thickness smaller than the theoretical maximum can be caused either by a tilting of the chemisorbed molecules or by conformational defects (deviation from all-*trans* conformation). Information on such defects can be gained by analysis of some vibrational bands, *e.g.* the one of the asymmetric CH_2 stretch mode. In spectra of stretched-out alkyl chains, this mode has wavenumber maxima at 2920 cm^{-1} and below, while for disordered chains, the band undergoes a marked blue shift.[24] The maximum of the asymmetric CH_2 stretch band in spectrum b (SAM of substance **7**) lies at 2920 cm^{-1}, indicating that the alkyl chain in the SAM is rather well-ordered. Analysis of the ethylene glycol CH_2 wagging band provides information on the conformation of the OEG chain in the SAM of substance **7**. The band maximum is at 1351 cm^{-1} which leads to the conclusion that the conformation of this chain is mainly *gauche*.[25] This finding is a possible explanation for an experimentally derived layer thickness that is clearly smaller than the maximum possible length of molecule **7** as

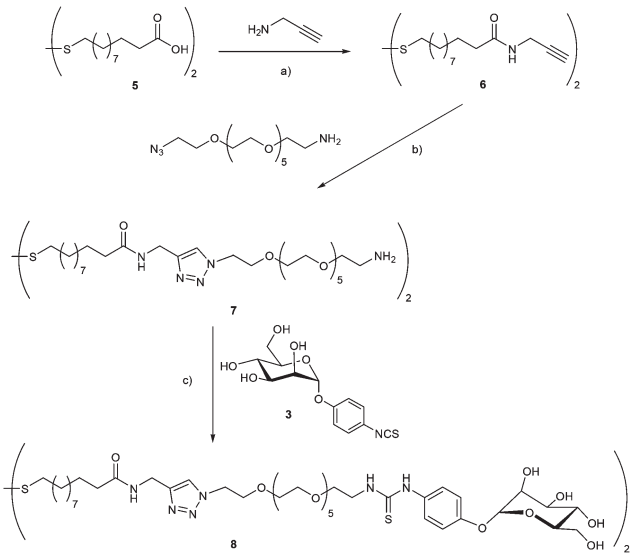

Scheme 3 Synthesis of amino-functionalised disulphide **7** and thiourea-bridging in solution. (a) HATU, DIPEA, DMF, 0 °C → rt, 6.5 h, 80%; (b) CuI, MeOH, 40 °C, 18 h, 78%; (c) DIPEA, THF, DMSO, 40 °C, 16 h, 62%.

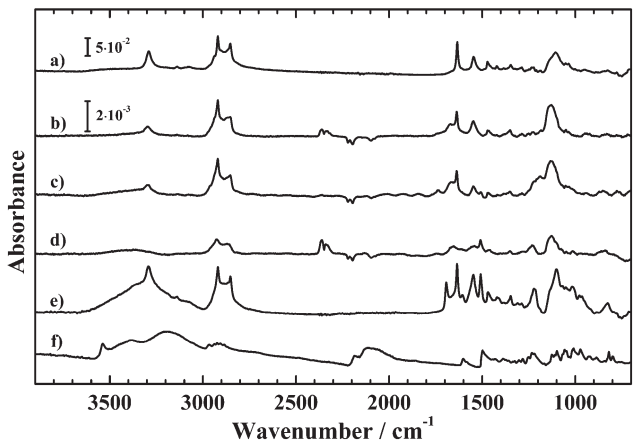

Fig. 1 FT-IR spectra of glyco-SAMs after different fabrication stages and of the involved neat substances. (a) IR spectrum of neat substance **7**, recorded with an ATR unit, (b) IRRA spectrum of **7**, after deposition onto an Au surface, (c) IRRA spectrum of the same sample as in b, but after surface thiourea-coupling with **3**, (d) IRRA spectrum of an Au surface after direct deposition of **4**, (e) FT-IR spectrum of neat substance **4**, recorded with an ATR unit, (f) FT-IR spectrum of neat substance **3**, recorded with an ATR unit. The absorbance scale for all ATR spectra (a, e, f) is indicated by the bar next to spectrum a. The absorbance scale for all monolayer spectra (b, c, d) is indicated by the bar next to spectrum b. Note that some negative and positive bands between 2000 and 2400 cm^{-1} in the **7**-SAM spectrum (trace b) as well as in both other SAM spectra are due to gas phase CO_2 in the spectrometer beam path and due to the perdeuterated alkanethiol SAM used as a reference.

reaching the full length requires all-*trans* conformation. Since OEG units with a *gauche* conformation have been associated with biorepulsivity, it could be expected that the SAM of **7** has this desired property.[26]

The next step in our 'dual click' strategy was the thiourea-coupling reaction to build up a layer of **8** as described above. After the coupling reaction of the SAM of **7** with mannoside **3**, three new bands appear in the IR spectrum of the resulting SAM (trace c), which can also be found in the bulk spectrum (trace e) of the acetyl-protected thiol **4**. Firstly, a broad signal between 3400 and 3600 cm^{-1} indicates the presence of OH groups which belong to the mannose moiety. This signal occurs in the monolayer spectrum of **8** (c) as well as in the spectra of neat substances **3** (f) and **4** (e). The second new signal is located at 1508 cm^{-1} in the spectrum of the SAM of **8** (c) and can be assigned to a CH bending mode in the aromatic ring (1498 and 1508 cm^{-1} in the spectra of neat substances **3** (f) and **4** (e)). The third new signal in the monolayer spectrum of **8** lies at 1188 cm^{-1} and is not present in the spectra of neat substances **3** and **7**, yet at 1222 cm^{-1} in the spectrum (e) of **4**. This band can be assigned to the stretch mode of the CS double bond formed in the thiourea-bridging reaction, thus demonstrating that the latter has been successful. This is corroborated by an increase of the layer thickness as measured by ellipsometry. After the thiourea-bridging step the SAM has a thickness of 34.8 ± 0.7 Å. Since molecule **3** has a length of approximately 11 Å, a greater increase would have been expected. We speculate that only a part of the NH_2 moieties exhibited by the **7** SAM reacted with substance **3**, leading only to a 5 Å increase of the average layer thickness.

For reasons of comparison, a 'conventional' SAM has been prepared by immersion of an Au substrate into a solution of substance **4** (corresponding to route E in Scheme 1) and characterised by IR spectroscopy and ellipsometry. The IRRA spectrum of the 'conventional' SAM of **4** (d) exhibits several bands that can also be found in the respective neat substance spectrum (e), *e.g.* the OH stretch band (3300–3600 cm^{-1}), the amide I and II bands (1653 and 1541 cm^{-1}) and the OEG CO band (1128 cm^{-1}). The missing acetyl CO stretch band (located at 1693 cm^{-1} in the neat substance spectrum (f) indicates removal of the acetyl unit upon S–Au bond formation, as expected. The layer thickness of this sample is 32 ± 1 Å which is somewhat smaller than the thickness of the 'clicked' SAM. The asymmetric CH stretch band of the 'conventional' SAM spectrum lies at a rather high wavenumber (2926 cm^{-1}), leading to the assumption of a mainly disordered alkylic chain in this SAM. From the lower overall IR signal intensity compared to the spectrum of the 'clicked' SAM (trace c) and from the smaller layer thickness, a lower concentration of molecules at the substrate surface can be inferred, which also points to a rather disordered monolayer.

In conclusion it can be stated that the thiourea 'click reaction' of the **7** SAM with substance **3** leads to a denser, better ordered mannose-terminated OEG SAM than the direct deposition of substance **4** onto the Au substrate.

Bacterial adhesion experiments

As mentioned in the introduction, the aim of this project was to develop a strategy permitting the selective adhesion of bioentities, such as bacteria. For this, the surfaces need not only to expose recognisable binding groups but also possess a generally biorepulsive background. Due to the 'dual click' strategy

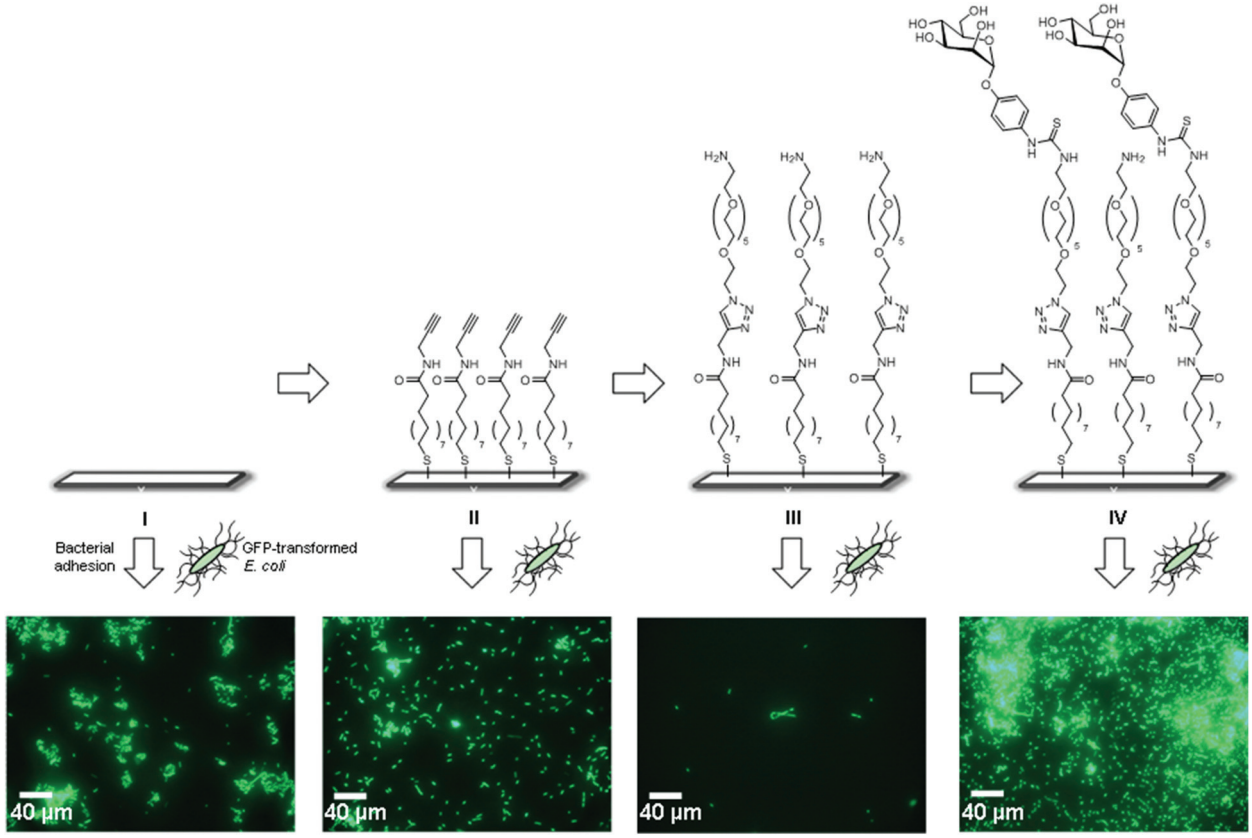

Scheme 4 Adhesion of fluorescent bacteria to the different stages of the SAM during the 'dual click' approach. The GFP-transformed *E. coli* bacteria (pPKL1162) enable a fast, direct fluorescence readout to investigate bacterial adhesion on surfaces. The native gold surface (I) was used as reference in each of the other experiments. As can be seen in the epifluorescence micrographs, the (non-specific) adhesivity of the alkyne-terminated SAM II is comparable to the one of the native Au surface. Introduction of the OEG chain reduces the adhesion significantly, while the α-mannosyl-terminated SAM is effectively recognised by the *E. coli* leading to heavy adhesion.

presented here, all three parts of such a monolayer can be tested sequentially. As a probe we decided to use GFP-tagged *E. coli* cells (strain pPKL1162), which expose multiple copies of type 1 fimbriae at their surface (Scheme 4). The lectin FimH, located at the termini of these fimbriae, is sensitive to α-D-mannosides and therefore ideally suited to demonstrate the biorelevance of the glyco-SAM. For this, the three stages of the SAM as well as pristine gold surfaces were exposed to suspensions of the bacteria for two hours each. The undecorated gold wafer (Scheme 4, I) and the alkyne-terminated surface (**1**, Scheme 4, II) were used to control unspecific binding of the fluorescent *E. coli* bacteria. Furthermore, adhesion studies were performed on the biorepulsive amino-terminated SAM (**7**, Scheme 4, III) and on the thiourea-bridged mannose-terminated glyco-SAM (**8**, Scheme 4, IV). After fluorescence detection of the GFP-tagged *E. coli* it emerged that the bacteria adhere with similar affinities to both control surfaces (Scheme 4, I and II) by unspecific binding events. On the other hand, the biorepulsive amino-terminated surface of deposited **7** (Scheme 4, III) indicated no significant bacterial adhesion due to the biorepulsive behaviour of the OEG moiety. After thiourea-bridging the mannose-specific FimH-mediated bacterial adhesion provided a high density of adhered bacteria on the glyco-SAM (**8**, Scheme 4, IV).

Adhesion was determined by counting the number of sessile bacteria per cm^2 after gentle purging of the surfaces. As can be seen in Fig. 2, the adhesion at the alkyne-terminated SAM of **1** (II) is comparable to the one at blank gold substrates (I, used as a reference), which suggests non-specific interactions. This interaction becomes effectively diminished for the amino-OEG-terminated SAM (II) indicating its biorepulsivity. In contrast to this, the mannose-terminated surface III, after the thiourea-bridging step, is significantly more adhesive for the *E. coli* strain used in this study. The number of adherent bacteria on this surface is three times the one on bare gold, indicating a specific binding mechanism.

With this, not only the successful attachment of the mannosyl moieties at the surface of the SAM could be demonstrated, but the viability of the 'dual click' approach as such. As a result of the fluorescence microscopic investigation of the bacterial adherence we can conclude that the type 1 fimbriae-mediated bacterial adhesion only occurs on the mannose-terminated glyco-SAM. As expected, the bacterial adhesion is negative for the biorepulsive control experiments.

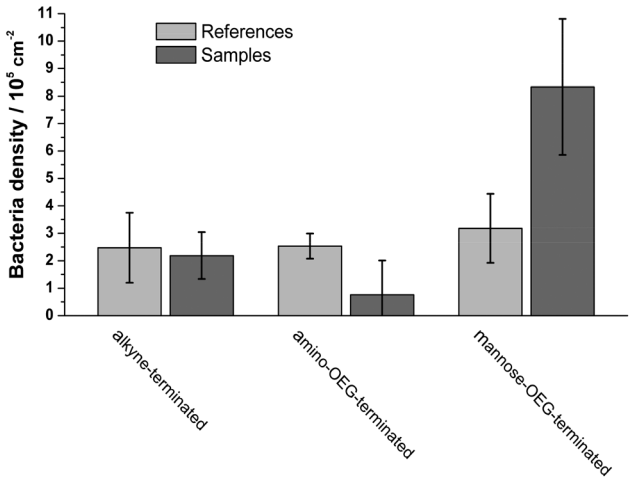

Fig. 2 Absolute bacteria density as determined by fluorescence microscopy on differently functionalised SAMs (samples) in comparison to bare gold surface substrates (references). Bacteria density data of alkyne-terminated, amino-OEG-terminated, and mannose-OEG-terminated SAMs refer to gold surfaces functionalised with **1**, **7**, and **8**, respectively.

Conclusions

In conclusion, it could be demonstrated that the 'dual click' strategy provides an excellent tool to produce glyco-SAMs suitable for bacteria-based assays. The use of two 'click reactions' instead of one permits also the alteration of the biorepulsive element between the basic SAM and the recognition site, so that the system can easily become adopted to the respective needs depending on the assay. This provides a new dimension in the toolbox for the fabrication of glycoarrays.

The possibility to thoroughly characterise the SAM-based systems in each of the construction steps (*e.g.* by IRRAS and ellipsometry) permits the optimisation of the individual 'click reactions' and also detecting unexpected pit-falls, such as the migration of protective groups previously considered as 'innocent'. We could also demonstrate that the SAMs formed by the sequential build-up on the surface are denser, at least at their basis, than those formed from long, completely preassembled molecules, making them also more stable. As a first test for the suitability of these systems for bio-assays with living bacteria, we could demonstrate that the introduction of the biorepulsive OEG-moiety not only suppressed the unspecific adsorption of *E. coli*, but also that the final attachment of the α-D-mannopyranoside enables the recognition of the surface by the bacteria.

Our investigations currently focus on extending this approach, *e.g.* for the fabrication of 'mixed type' SAMs exposing more than one receptor molecule, the synthesis of photoswitchable systems as well as the extension to true arrays with many different surface chemistries on one substrate. These systems will then be tested for their interactions with lectins and, in particular, living cells.

Experimental section

General remarks

Commercially available starting materials were used without further purification: *p*-nitrophenyl α-D-mannopyranoside (*p*NPMan) was purchased from Senn Chemicals, 11-mercapto-undecanoic acid and propargylamine were from Aldrich, *N*-Boc-ethylenediamine was from ABCR and amino-hexaethylene glycol azide was from Polypure. Solvents were purified by distillation prior to use. Reaction monitoring was performed by TLC on silica gel F_{254} (Merck) or RP-18 (Merck) plates, detection was achieved by UV light and/or by treatment of the plates with a vanillin solution [vanillin (1.00 g) in methanol (100 mL) and addition of glacial acetic acid (12.0 mL) and sulphuric acid (4.00 mL)] or ninhydrin solution [ninhydrin (300 mg) in butanol (100 mL) and glacial acetic acid (3.00 mL)] and subsequent heating. Flash chromatography was performed on Merck silica gel 60 (0.040–0.063 mm). For NMR spectroscopy Bruker DRX 500 or AV 600 instruments were used. Chemical shifts (δ) are calibrated relative to the internal solvent. For complete assignment the following two-dimensional NMR techniques were used: ^{1}H–^{1}H COSY, ^{1}H–^{13}C HSQC and ^{1}H–^{13}C HMBC. ESI-MS measurements were performed on a Mariner instrument, MALDI-TOF mass spectra were recorded with a Bruker Biflex III instrument with 19 kV acceleration voltage and an ionization laser at 337 nm; 4-chloro-α-cyanocinnamic acid (Cl-CCA) was used as a matrix. Optical rotation values were measured on a Perkin-Elmer 241 polarimeter (10 cm cells, Na-D-line: 589 nm) and are averaged from five measurements. Elemental analyses were carried out with a EuroEA3000 Elemental Analyzer from EuroVector.

N-[(20-Amino-hexaethylene glycolyl)-1*H*-[1,2,3]-triazole-4-yl-methyl]-11-thioacetyl-undecanoic acid amide (2)

Thioacetate **1** (74 mg, 211 μmol) and amino-hexaethylene glycol azide (63 mg, 211 μmol) were dissolved in degassed MeCN (3 mL), CuI (7.9 mg, 42 μmol, 0.2 eq.) was added and the reaction mixture was stirred for 24 h at 45 °C. After removing the copper salt by filtration, the crude product was purified by flash chromatography ($CHCl_3$–MeOH 7 : 1) and lyophilised to obtain **2** (61 mg, 94 μmol, 46%) as a colourless substance. ^{1}H NMR (600 MHz, MeOH-d_4): δ 7.87 (s, 1H, H-15), 4.58 (t, 2H, J = 5.1 Hz, H-14), 4.42 (s, 2H, H-17), 3.89 (t, 2H, J = 5.1 Hz, H-13), 3.72–3.59 (m, 22H, H-2–H-12), 3.09 (t, 2H, J = 5.1 Hz, H-1), 2.86 (t, 2H, J = 7.4 Hz, H-28), 2.30 (s, 3H, H-30), 1.21 (t, 2H, J = 7.4 Hz, H-19), 1.61 (m_c, 2H, H-27), 1.55 (quint, 2H, J = 7.4 Hz, H-20), 1.38–1.27 (m, 12H, H-21–H-26) ppm; ^{13}C NMR (150 MHz, MeOH-d_4): δ 197.6 (C-29), 176.2 (C-28), 146.3 (C-16), 124.9 (C-15), 71.6–70.8 (CH_2OCH_2), 67.9 (C-13), 51.3 (C-14), 40.5 (C-1), 36.9 (C-19), 35.6 (C-17), 30.8 (C-20), 30.5 (C-30), 30.3–29.8 (C-20–C-26, C-28), 26.9 (C-27) ppm; ESI MS: $[M + H]^+$ m/z calcd for $C_{30}H_{58}N_5O_8S$: 648.400; found: 648.397.

N-{20-[*p*-(α-D-Mannopyranosyloxy)-phenylthioureido-hexaethylene glycolyl]-1*H*-[1,2,3]-triazole-4-yl-methyl}-11-thioacetyl-undecanoic acid amide (4)

The amine **2** (3.9 mg, 6.0 μmol) was dissolved in dry DMF (2 mL) and treated with isothiocyanatophenyl mannoside **3** (3.8 mg, 12 μmol, 2.0 eq.) and DIPEA (2.0 μL, 12 μmol, 1.9 eq.). The reaction solution was stirred at room temperature for 12 h, subsequently the solvent was removed *in vacuo*. The crude product was purified by column chromatography (ethyl acetate–MeOH 2 : 1) to obtain molecule **4** (5.7 mg, 6.0 μmol, quant.) as a colourless syrup. ^{1}H NMR (600 MHz, DMSO-d$_6$): δ 9.60 (br s, 1H, NH), 8.42 (br s, 1H, NH), 7.84 (s, 1H, H-26), 7.28 (d, 2H J = 8.9 Hz, aryl-H), 6.99 (d, 2H, J = 8.9 Hz, aryl-H), 5.29 (d, 1H, $J_{1,2}$ = 1.7 Hz, H-1$_{man}$), 4.99 (d, 1H, J = 4.1 Hz, OH), 4.84 (d, 1H, J = 5.4 Hz, OH), 4.73 (d, 1H J = 5.0 Hz, OH), 4.45 (t, 2H, J = 5.3 Hz, H-25), 4.42 (t, 1H, J = 6.0 Hz, OH), 4.26 (d, 2H, J = 5.6 Hz, H-28), 3.81 (m$_c$, 1H, H-2$_{man}$), 3.72 (t, 2H, J = 5.2 Hz, H-24), 3.65 (m$_c$, 1H, H-3$_{man}$), 3.63–3.56 (m, 3H, H-6a$_{man}$, H-12), 3.56–3.45 (m, 24H, H-4$_{man}$, H-6b$_{man}$, H-13–H-23), 3.41 (m$_c$, 1H, H-5$_{man}$), 2.81 (t, 2H, J = 7.2 Hz, H-38), 2.31 (s, 3H, H-40), 2.06 (t, 2H, J = 7.4 Hz, H-30), 1.48 (m$_c$, 4H, H-31, H-37), 1.31–1.19 (m, 10H, H-32–-36) ppm; ^{13}C NMR (125 MHz, DMSO-d$_6$): δ 195.8 (C-39), 180.9 (C-11), 172.5 (C-29), 153.8 (C-7), 145.4 (C-27), 131.5 (C-9), 123.5 (C-8), 117.4 (C-9), 99.7 (C-1$_{man}$), 75.4 (C-5$_{man}$), 71.1 (C-3$_{man}$), 70.6 (C-2$_{man}$), 70.2–69.1 (CH_2OCH_2), 67.2 (C-4$_{man}$), 61.5 (C-6$_{man}$), 49.7 (C-25), 35.7 (C-30), 34.5 (C-28), 31.0 (C-40), 29.56, 29.3, 29.2, 29.1, 28.9, 28.8, 28.6 (C-31–C-36), 25.7 (C-37) ppm; MALDI-ToF MS: $[M + H]^+$ m/z calcd for $C_{43}H_{73}N_6O_{14}S_2$: 961.4626; found: 961.6045; $[M + Na]^+$ calcd for $C_{43}H_{72}N_6O_{14}S_2Na$: 983.4446; found: 983.5957.

Bis-[*N*-(propynyl)-11,11′-disulphanediyl diundecanoic acid diamide (6)

To an ice-cold solution of dicarboxylic acid **5** (400 mg, 921 μmol) in dry DMF (10 mL) DIPEA (625 μL, 3.68 mmol, 4.0 eq.) was added and the reaction mixture stirred for 5 min. Afterwards, HATU (1.05 g, 2.76 mmol, 3.0 eq.) was added and after an additional 30 min of stirring, propargylamine (236 μL, 3.68 mmol, 4.0 eq.), dissolved in 3 mL dry DMF, was added dropwise. Then the reaction mixture was stirred for 6.5 h at room temperature. The precipitated product was subsequently filtered and washed with ice-cold DMF to obtain **6** (375 mg, 738 μmol, 80%) as a white solid. m.p.: 115 °C; ^{1}H NMR (500 MHz, DMSO-d$_6$): δ 8.08 (s, 2H, 2 NH), 3.83 (dd, 4H, J = 2.4 Hz, 4 H-3), 2.98 (s, 2H, 2 H-1), 2.69 (t, 4H, J = 7.2 Hz, 4 H-14), 2.07 (t, 4H, J = 7.4 Hz, 4 H-5), 1.61 (quint ∼ tt, 4H, J = 7.2 Hz, 4 H-13), 1.48 (m$_c$, 4H, 4 H-6), 1.34 (m$_c$, 4H, 4 H-12), 1.31–1.21 (m, 20H, H-7, H-8, H-9, H-10, H-11) ppm; ^{13}C NMR (125 MHz, DMSO-d$_6$): δ 172.3 (C-4), 81.8 (C-2), 72.9 (C-1), 38.6 (C-14), 35.6 (C-5), 29.3, 29.2, 29.1, 29.1, 29.0, 29.0 (C-7, C-8, C-9, C-10, C-11, C-13), 28.2 (C-3, C-12), 25.6 (C-6) ppm; EA: calcd for $C_{28}H_{48}N_2O_2S_2$ (M = 508.3157 g mol^{-1}): C 66.09, H 9.51, N 5.51, S 12.60; found: C 66.11, H 9.87, N 5.62, S 12.09.

Bis-{*N*-[(20-amino-hexaethylene glycolyl)-1*H*-[1,2,3]-triazole-4-yl-methyl]}-11,11′-disulphanediyl diundecanoic acid diamide (7)

The dialkyne **6** (35 mg, 69 μmol) and amino-hexaethylene glycol azide (48 mg, 138 μmol, 2.0 eq.) were dissolved in degassed MeOH (5 mL). After CuI (11 mg, 55 μmol, 0.8 eq.) was added, the reaction mixture was stirred at 40 °C for 18 h. The solvent was removed *in vacuo* and the crude product purified by flash chromatography ($CHCl_3$–MeOH 2 : 1 + 1% Et_3N) to obtain **7** (65 mg, 54 μmol, 78%) as a colourless solid. m.p. 103 °C; ^{1}H NMR (500 MHz, DMSO-d$_6$): δ 8.17 (br s, 2H, NH), 7.83 (br s, 2H, 2 H-15), 4.48 (t, 4H, J = 5.3 Hz, 4 H-14), 4.28 (d, 4H, J = 5.6 Hz, 4 H-17), 3.80 (t, 4H, J = 5.3 Hz, 4 H-13), 3.56–3.48 (m, 44H, H-2, H-3, H-4, H-5, H-6, H-7, H-8, H-9, H-10, H-11, H-12), 3.42 (m ∼ t, 4H, 2 NH$_2$), 2.73–2.66 (m, 8 H, H-1, H-28), 2.08 (t, 4H, J = 7.5 Hz, H-19), 1.61 (quint, 4H, J = 7.3 Hz, H-27), 1.49 (m$_c$, 4H, H-20), 1.34 (m$_c$, 4H, H-26), 1.27–1.21 (m, 20H, H-21, H-22, H-23, H-24, H-25) ppm; ^{13}C NMR (125 MHz, DMSO-d$_6$): δ 172.5 (C-18), 145.4 (C-16), 123.5 (C-15), 72.3–70.1 (C-2, C-3, C-4, C-5, C-6, C-7, C-8, C-9, C-10, C-11, C-12), 69.3 (C-13), 49.8 (C-14), 41.4 (C-1), 38.4 (C-28), 35.8 (C-19), 34.6 (C-17), 29.3, 29.2, 29.2, 29.1, 29.0, 29.0 (C-21, C-22, C-23, C-24, C-25, C-26), 28.2 (C-27), 25.7 (C-20) ppm; EA: calcd for $C_{56}H_{108}N_{10}O_{14}S_2$·3.5 H_2O (M = 1271.78 g mol^{-1}): C 52.85, H 9.11, N 11.01, S 5.04; found: C 53.10, H 8.72, N 10.25, S 4.18; MALDI-ToF MS: $[M + H]^+$ calcd for $C_{56}H_{109}N_{10}O_{14}S_2$: 1209.7566; found: 1210.0132; $[M + Na]^+$ calcd for $C_{56}H_{108}N_{10}O_{14}S_2Na$: 1231.7386; found: 1232.0632.

Bis-{*N*-[20-(*p*-(α-D-mannopyranosyloxy)-phenylthioureido-hexaethylene glycolyl]-1*H*-[1,2,3]-triazole-4-yl-methyl]}-11,11′-disulphanediyl diundecanoic acid diamide (8)

The diamine **7** (16 mg, 13 μmol) and mannoside **3** (8.4 mg, 26 μmol, 2.0 eq.) were dissolved in a mixture of THF and DMSO (2.5 mL, 4 : 1) and treated with DIPEA (5.0 μL, 27 μmol, 2.02 eq.). The reaction mixture was stirred for 48 h at 40 °C. After removing the solvent *in vacuo*, the crude product was purified by chromatography ($CHCl_3$–MeOH 5 : 1) to obtain **8** (14 mg, 8.0 μmol, 62%) as a colourless solid. $[\alpha]_D^{20}$ = +30.9 (c 0.23, DMSO); m.p. 78 °C; ^{1}H NMR (600 MHz, DMSO-d$_6$): δ 9.61 (br s, 2 H, NH), 8.26 (br s, 2H, NH), 7.86 (s, 2H, H-26), 7.68 (br s, 2H, NH), 7.29, 7.01 (each d, each 4H, J = 8.8 Hz, aryl-H), 5.33 (d, 2H, J = 1.3 Hz, H-1$_{man}$), 5.01 (d, 2H, J = 4.3 Hz, OH), 4.83 (d, 2H, J = 5.6 Hz, OH), 4.76 (d, 2H, J = 4.8 Hz, OH), 4.48 (d, 4H, J = 5.2 Hz, H-25), 4.45 (d, 2H, J = 6.0 Hz, OH), 4.26 (d, 4H, J = 5.2 Hz, H-28), 3.81 (m$_c$, 2H, H-2$_{man}$), 3.79 (t, 4H, J = 5.2 Hz, H-24), 3.66 (m$_c$, 2H, H-3$_{man}$), 3.64–3.55 (m, 6H, H-6a$_{man}$, H-12), 3.55–3.46 (m, 48H, H-4$_{man}$, H-6b$_{man}$, H-13–H-23), 3.41 (m$_c$, 2H, H-5$_{man}$), 2.68 (t, 4H, J = 7.2 Hz, H-39), 2.07 (t, 4H, J = 7.4 Hz, H-30), 1.60 (quint, 4H, J = 7.2 Hz, H-38), 1.48 (m$_c$, 4H, H-31), 1.33 (m$_c$, 4H, H-37), 1.26–1.20 (m, 20H, H-32–H-36) ppm; ^{13}C NMR (150 MHz, DMSO-d$_6$): δ 180.7 (C-11), 172.0 (C-29), 153.4 (C-7), 144.9 (C-27), 133.4 (C-10), 125.0 (C-8), 123.0 (C-26), 116.9 (C-9), 99.3 (C-1$_{man}$), 74.9 (C-5$_{man}$), 70.7 (C-3$_{man}$), 70.1 (C-2$_{man}$), 69.8–68.6 (CH_2OCH_2), 66.9 (C-4$_{man}$),

61.0 (C-6_{man}), 49.3 (C-25), 43.5 (C-12), 37.8 (C-39), 35.2 (C-30), 34.1 (C-28), 28.9–28.5 (CH_2), 27.7 (C-37), 25.2 (C-31) ppm; EA: calcd for $C_{82}H_{138}N_{12}O_{26}S_4 \cdot 7.6\ H_2O \cdot 1.2$ DMSO (M = 2065.50 g mol^{-1}): C 49.04, H 7.82, N 8.14, S 8.07; found: C 49.10, H 7.24, N 7.65, S 7.99; MALDI-ToF MS: $[M + H]^+$ calcd for $C_{82}H_{139}N_{12}O_{26}S_4$: 1837.3059; found: 1837.0693; $[M + Na]^+$ calcd for $C_{82}H_{138}N_{12}O_{26}S_4Na$: 1859.2877; found: 1859.1165.

Gold substrate preparation

Silicon wafers (100) coated with 10 nm of chromium and 200 nm of gold (111) were cut into small pieces of about 15 × 20 mm^2 size. For ellipsometry measurements, four small regions on the gold substrates were marked with circles using a sharp tip. The substrates were then rinsed with pure ethanol and dried in a nitrogen stream, before chemisorbed contaminants were removed using hydrogen plasma (hydrogen pressure: 0.5 Pa, 25 W, 2 min).[27]

Self-assembled monolayer preparation

Self-assembled monolayers were prepared by immersion of gold substrates into solutions of the respective organodisulphides or thioacetates. Dimethylformamide p.a. was used as a solvent for all solutions except for molecule **1**, which was deposited from solution in tetrahydrofuran. Concentrations were 0.02 mM in the case of molecule **7** and 0.03 mM in the case of molecule **3**. If the solutions were not completely clear, they were filtered through a syringe filter (polytetrafluoroethylene, 0.2 μm pore diameter). The concentration of **1** amounted to 0.2 mM; an equimolar amount of NH_4OH was added to promote the cleavage of the *S*-acetyl group. All solvents were used without further purification. Immersion times varied between 15 and 22 h. After removal from the solutions, the samples were thoroughly rinsed with the respective solvent used for the deposition, then rinsed with ethanol, and blown dry in an argon stream.

Thiourea-bridging on surface

Gold substrate samples functionalised with molecule **7** (OEG-amino-terminated SAM) were immersed into solutions of molecule **3** (5 mM) and DIPEA (15 mM) in THF (p.a.). The substrates remained in the solutions at ambient air and 40 °C in a shaker for 15–60 h. Afterwards, the samples were taken out of the solution, rinsed with ethanol, blown dry with an Ar or N_2 stream and characterised by IRRAS and ellipsometry.

Ellipsometry

The thickness of the SAMs after preparation and after surface 'click reactions' was measured with a Sentech SE 400 ellipsometer equipped with a He Ne laser (wavelength 632.8 nm, beam diameter 1–2 mm). The angle of incidence amounted to 70° with respect to the sample surface normal.

Complex refraction indices of the gold substrates were measured at four labeled positions per substrate before the latter were immersed into the disulphide or thioacetate solutions. The extinction coefficients of the monolayers before and after 'click reactions' were assumed to be zero. The refractive indices were in all cases assumed to be 1.37, a value that represents a good compromise for molecules with OEG moieties.

Infrared measurements

IR spectra of neat substances were recorded using a Nicolet 6700 Fourier transform IR spectrometer with a liquid nitrogen-cooled narrow-band mercury cadmium telluride (MCT) detector equipped with an ATR unit and with a Perkin-Elmer 1600 Series FT-IR spectrometer equipped with an MKII Golden Gate™ Single Reflection ATR A-531-G unit. The Nicolet spectrometer was also employed to characterise the freshly prepared SAMs and the SAMs after execution of the surface 'click reactions' using an infrared reflection absorption spectroscopy (IRRAS) sample holder. Its beam path was purged with dry and CO_2-free air throughout the measurements. IRRA spectra were recorded with *p*-polarised IR radiation in grazing-incidence at an angle of 80° with respect to the sample surface normal. SAMs of perdeuterated dodecanethiol on Au were used as a reference for the IRRAS measurements. All spectra were acquired at a resolution of 4 cm^{-1}. In the IRRAS experiments, 512 scans were performed to improve the signal to noise ratio, followed by smooth baseline correction.

Bacteria adhesion experiments

Fluorescent GFP-tagged *E. coli* (pPKL1162) with resistance to ampicillin and chloramphenicol were used for bacteria adhesion tests on gold substrate surfaces functionalised with molecules **1**, **7**, and **8**. Suspensions of the bacteria in CASO broth with an optical density of 0.5 (which corresponds to *ca.* 6 × 10^8 bacteria per cm^3) were used. For each kind of functionalised surface, five specimens were used. Equivalent numbers of bare gold surfaces were used as references. Prior to bacteria adhesion, all samples were sterilised by thorough rinsing with ethanol and heating to 45 °C for one hour. Adsorption experiments were carried out for 2 hours at 37 °C in a shaker at 200 rpm, using 20 mL of the bacteria suspension per sample. Afterwards, the samples were dipped into Falcon tubes with 20 mL PBS solution and shaken at 200 rpm for one minute. Subsequently they were immersed in a beaker with sterile PBS (phosphate buffered saline) solution, and after removal from the solution and drip drying, they were mounted onto microscope slides.

The numbers of bacteria per cm^2 were determined using a Horiba microscope fluorescence lifetime imaging system, combined with an Olympus DX 5 optical microscope, running in fluorescence microscopy mode and equipped with a Lumen Dynamics X-Cite 120 Q mercury vapor short arc lamp. On each sample, ten different locations with an area of 0.14 mm^2 each were randomly chosen for bacteria counting.

Acknowledgements

This work was financed by the DFG (SFB 677). Part of the work was supported by the Beilstein-Institut, Frankfurt/Main, Germany, within the research collaboration NanoBiC.

Notes and references

1 (*a*) A. Varki, *Glycobiology*, 1993, **3**, 97–130; (*b*) R. A. Dwek, *Chem. Rev.*, 1996, **96**, 683–720; (*c*) H.-J. Gabius, H.-C. Siebert, S. André, J. Jiménez-Barbero and H. Rüdiger, *ChemBioChem*, 2004, **5**, 740–764; (*d*) J. C. Paulson, O. Blixt and B. E. Collins, *Nat. Chem. Biol.*, 2006, **2**, 238–248.

2 (*a*) L. L. Kiessling and R. A. Splain, *Annu. Rev. Biochem.*, 2010, **79**, 619–653; (*b*) C.-Y. Wu and C.-H. Wong, *Chem. Commun.*, 2011, **47**, 6201–6207.

3 (*a*) M. Mrksich, *Chem. Soc. Rev.*, 2000, **29**, 267–273; (*b*) M. C. Bryan, O. Plettenburg, P. Sears, D. Rabuka, S. Wacowich-Sgarbi and C.-H. Wong, *Chem. Biol.*, 2002, **9**, 713–720; (*c*) S. Fukui, T. Feizi, C. Galustian, A. M. Lawson and W. Chai, *Nat. Biotechnol.*, 2002, **20**, 1011–1017; (*d*) D. M. Ratner, E. W. Adams, J. Su, B. R. O'Keefe, M. Mrksich and P. H. Seeberger, *ChemBioChem*, 2004, **5**, 379–383; (*e*) T. Horlacher and P. H. Seeberger, *Chem. Soc. Rev.*, 2008, **37**, 1414–1422; (*f*) N. Laurent, J. Voglmeir and S. Flitsch, *Chem. Commun.*, 2008, 4400–4412; (*g*) O. Oyelaran and J. C. Gildersleeve, *Curr. Opin. Chem. Biol.*, 2009, **13**, 406–413; (*h*) C. Rillahan and J. C. Paulson, *Annu. Rev. Biochem.*, 2011, **80**, 797–823; (*i*) C. Grabosch, K. Kolbe and T. K. Lindhorst, *ChemBioChem*, 2012, **13**, 1874–1879; (*j*) J. Wehner, M. Weissenborn, M. Hartmann, C. J. Gray, R. Šardzik, C. E. Eyers, S. L. Flitsch and T. K. Lindhorst, *Org. Biomol. Chem.*, 2012, **10**, 8919–8926; (*k*) S. Park, J. C. Gildersleeve, O. Blixt and I. Shin, *Chem. Soc. Rev.*, 2013, DOI: 10.1039/C2CS35401B.

4 (*a*) B. T. Houseman and M. Mrksich, *Chem. Biol.*, 2002, **9**, 443–454; (*b*) M. Kleinert, T. Winkler, A. Terfort and T. K. Lindhorst, *Org. Biomol. Chem.*, 2008, **6**, 2118–2132; (*c*) L. Ban and M. Mrksich, *Angew. Chem.*, 2008, **47**, 3444–3447, (*Angew. Chem., Int. Ed.*, 2008, **47**, 3396–3399); (*d*) N. Laurent, R. Haddoub, J. Voglmeir, S. C. C. Wong, S. J. Gaskell and S. L. Flitsch, *ChemBioChem*, 2008, **9**, 2592–2596; (*e*) F. Tantakitti, J. Burk-Rafel, F. Cheng, R. Egnatchik, T. Owen, M. Hoffmann, D. N. Weiss and D. M. Ratner, *Langmuir*, 2012, **28**, 6950–6959.

5 (*a*) J. C. Love, L. A. Estroff, J. K. Kriebel, R. G. Nuzzo and G. M. Whitesides, *Chem. Rev.*, 2005, **105**, 1103–1169; (*b*) Z.-L. Zhi, N. Laurent, A. K. Powell, R. Karamanska, M. Fais, J. Voglmeir, A. Wright, J. M. Blackburn, P. R. Crocker, D. A. Russell, S. Flitsch, R. A. Field and J. E. Turnbull, *ChemBioChem*, 2008, **9**, 1568–1575.

6 B. T. Houseman and M. Mrksich, *Chem. Biol.*, 2002, **9**, 443–454.

7 (*a*) M. Kind and C. Wöll, *Prog. Surf. Sci.*, 2009, **84**, 230–278; (*b*) K. A. Barth, G. Coullerez, L. M. Nilsson, R. Castelli, P. H. Seeberger, V. Vogel and M. Textor, *Adv. Funct. Mater.*, 2008, **18**, 1459–1469; (*c*) Z. A. Gurard-Levin and M. Mrksich, *Annu. Rev. Anal. Chem.*, 2008, **1**, 767–800.

8 (*a*) M. C. Fritz, G. Hähner, N. D. Spencer, R. Bürli and A. Vasella, *Langmuir*, 1996, **12**, 6074–6082; (*b*) D. J. Revell, J. R. Knight, D. J. Blyth, A. H. Haines and D. A. Russell, *Langmuir*, 1998, **14**, 4517–4524; (*c*) M. Mrksich, C. S. Chen, Y. Xia, L. E. Dike, D. E. Ingber and G. M. Whitesides, *Proc. Natl. Acad. Sci. U. S. A.*, 1996, **93**, 10775–10778.

9 (*a*) M. Kleinert, N. Röckendorf and T. K. Lindhorst, *Eur. J. Org. Chem.*, 2004, 3931–3940; (*b*) M. I. Bethencourt, L. Srisombat, P. Chinwangso and T. R. Lee, *Langmuir*, 2009, **25**, 1265–1271.

10 (*a*) M. R. Lockett, M. F. Phillips, J. L. Jarecki, D. Peelen and L. M. Smith, *Langmuir*, 2008, **24**, 69–75; (*b*) E. Locatelli, G. Ori, M. Fournelle, R. Lemor, M. Montorsi and M. C. Franchini, *Chem.–Eur. J.*, 2011, **17**, 9052–9056.

11 (*a*) K. L. Prime and G. M. Whitesides, *Science*, 1991, **252**, 1164–1167; (*b*) R. Chelmowski, S. D. Köster, A. Kerstan, A. Prekelt, C. Grunwald, T. Winkler, N. Metzler-Nolte, A. Terfort and C. Wöll, *J. Am. Chem. Soc.*, 2008, **130**, 14952–14953; (*c*) S. Herrwerth, W. Eck, S. Reinhardt and M. Grunze, *J. Am. Chem. Soc.*, 2003, **125**, 9359–9366; (*d*) K. L. Prime and G. M. Whitesides, *J. Am. Chem. Soc.*, 1993, **115**, 10714–10721.

12 (*a*) W. I. Weis and K. Drickamer, *Annu. Rev. Biochem.*, 1996, **65**, 441–473; (*b*) H. Lis and N. Sharon, *Chem. Rev.*, 1998, **98**, 637–674.

13 M. Ambrosi, N. R. Cameron and B. G. Davis, *Org. Biomol. Chem.*, 2005, **3**, 1593–1608.

14 K. Ohlsen, T. A. Oelschlaeger, J. Hacker and A. Salam Khan, *Top. Curr. Chem.*, 2009, **288**, 17–65.

15 A. Reisner, K. A. Krogfelt, B. M. Klein, E. L. Zechner and S. Molin, *J. Bacteriol.*, 2006, **188**, 3572–3581.

16 G. G. Anderson, K. W. Dodson, T. M. Hooton and S. J. Hultgren, *Trends Microbiol.*, 2004, **12**, 424–430.

17 (*a*) X. Jiang, D. Abgottspon, S. Kleeb, S. Rabbani, M. Scharenberg, M. Wittwer, M. Haug, O. Schwardt and B. Ernst, *J. Med. Chem.*, 2012, **55**, 4700–4713; (*b*) M. Hartmann, H. Papavlassopoulos, V. Chandrasekaran, C. Grabosch, F. Beiroth, T. K. Lindhorst and C. Röhl, *FEBS Lett.*, 2012, **586**, 1459–1465; (*c*) C. Grabosch, M. Hartmann, J. Schmidt-Lassen and T. K. Lindhorst, *ChemBioChem*, 2011, **12**, 1066–1074.

18 M. Hartmann, A. K. Horst, P. Klemm and T. K. Lindhorst, *Chem. Commun.*, 2010, **46**, 330–332.

19 M. Hartmann and T. K. Lindhorst, *Eur. J. Org. Chem.*, 2011, 3583–3609.

20 (*a*) D. Choudhury, A. Thompson, V. Stojanoff, S. Langermann, J. Pinkner, S. J. Hultgren and S. D. Knight, *Science*, 1999, **285**, 1061–1066; (*b*) C.-S. Hung, J. Bouckaert, D. Hung, J. Pinkner, C. Widberg, A. DeFusco, C. G. Auguste, R. Strouse, S. Langermann, G. Waksman and S. J. Hultgren, *Mol. Microbiol.*, 2002, **44**, 903–915; (*c*) J. Bouckaert, J. Berglund, M. Schembri, E. De Genst, L. Cools, M. Wuhrer, C.-S. Hung, J. Pinkner, R. Slättegärd, A. Zavialov, D. Choudhury, S. Langermann, S. J. Hultgren, L. Wyns, P. Klemm, S. Oscarson, S. D. Knight and H. De Greve, *Mol. Microbiol.*, 2005, **55**, 441–455; (*d*) A. Wellens, C. Garofalo, H. Nguyen, N. Van Gerven, R. Slättegärd, J. P. Hernalsteens, L. Wyns, S. Oscarson, H. De Greve, S. Hultgren and J. Bouckaert, *PLoS One*, 2008, **3**, e2040; (*e*) Z. Han, J. S. Pinkner, B. Ford, R. Obermann, W. Nolan, S. A. Wildman,

D. Hobbs, T. Ellenberger, C. K. Cusumano, S. J. Hultgren and J. W. Janetka, *J. Med. Chem.*, 2010, **53**, 4779–4792.

21 (*a*) C. Grabosch, M. Kleinert and T. K. Lindhorst, *Synthesis*, 2010, 828–836; (*b*) M. Kleinert, T. Winkler, A. Terfort and T. K. Lindhorst, *Org. Biomol. Chem.*, 2008, **6**, 2118–2132.

22 (*a*) C. W. Tornøe, C. Christensen and M. Meldal, *J. Org. Chem.*, 2002, **67**, 3057–3064; (*b*) V. V. Rostovtsev, L. G. Green, V. V. Fokin and K. B. Sharpless, *Angew. Chem., Int. Ed.*, 2002, **41**, 2596–2599.

23 D. H. Buss and I. J. Goldstein, *J. Chem. Soc.*, 1968, **12**, 1457–1461.

24 (*a*) R. G. Snyder, H. L. Strauss and C. A. Elliger, *J. Phys. Chem.*, 1982, **86**, 5145–5150; (*b*) R. A. MacPhail, H. L. Strauss, R. G. Snyder and C. A. Elliger, *J. Phys. Chem.*, 1984, **88**, 334–341.

25 (*a*) H. Matsuura and T. Miyazawa, *Bull. Chem. Soc. Jpn.*, 1986, **41**, 1798–1808; (*b*) H. Matsuura and T. Miyazawa, *J. Polym. Sci.*, 1969, **7**, 1735–1744.

26 P. Harder, M. Grunze, R. Dahint, G. M. Whitesides and P. E. Laibinis, *J. Phys. Chem. B*, 1998, **102**, 426–436.

27 K. Raiber, A. Terfort, C. Benndorf, N. Krings and H. H. Strehblow, *Surf. Sci.*, 2005, **595**, 56–63.